

Measurement Analysis of Non-Invasive Blood Glucose On Sensor Coplanar Waveguide Loaded Square Ring Resonator with Interdigital Coupling Capacitor

Catur Ratmoko ^{a,*}, Iryanto Laisa ^b, Mudrik Alaydrus ^a

^a Electrical Department, Faculty of Engineering, Mercu Buana University, Jakarta, Indonesia

^b College of Shipping Science, Marunda Makmur, North Jakarta, 14150, Indonesia

Corresponding author: *caturratmoko@gmail.com

Abstract— This study presents the experimental results of a system with a sensor structure detecting human blood glucose levels. A microwave-based sensor is used for non-invasive blood glucose monitoring. The sensor design uses an asymmetrically loaded CPW structure as a square ring resonator with an interdigital coupling capacitor on the ground side. Simulated with a load of artificial finger tissue made from gelatin, modeled in four layers. The first layer is the skin is the outermost tissue, the next layer is fat, blood and bone. Each layer of tissue has a certain thickness size; skin (0.3mm), fat (0.2mm), blood (1.5mm), and bone (4mm). The measurement simulation is used, HFSS as modeling simulation and VNA as a measurement of the physical representation of the design results with parametric optimization methods. To verify the correlation and the expected sensitivity, media with different dielectrics were mounted on the surface of the sensor resonator with blood glucose levels of 1mg/dl, 72mg/dl, 126mg/dl, 162mg/dl and 216mg/dl. Reflection factor S_{11} was observed based on dielectric constant blood glucose levels (dB) fluctuations. Analysis of the data on the graph between the independent variables, namely blood glucose concentration and the dependent variable levels of S_{11} has an “R” correlation value of 0.97. The sensitivity level of the sensor on the S_{11} reflection factor with HFSS simulation averages 73.36mdB/mgdl⁻¹ and VNA reaches 82.39mdB/mgdl⁻¹. The results are interesting for developing a more optimal glucose sensor system.

Keywords— Sensor; grounded of CPW; resonator loaded ground structure; square ring resonator with interdigital coupling capacitor; non-invasive measurement of blood glucose levels.

Manuscript received 13 Feb. 2023; revised 15 Sep. 2023; accepted 27 Oct. 2023. Date of publication 31 Dec. 2023.
IJASEIT is licensed under a Creative Commons Attribution-Share Alike 4.0 International License.



I. INTRODUCTION

Currently, many diseases are caused by unhealthy lifestyles, one of which is diabetes. In medicine, known as Diabetes Mellitus (DM), it is a disease that occurs due to too high levels of blood glucose in a person's body. According to data from the World Health Organization (WHO), the number of people with diabetes in Indonesia will increase from 8.4 million in 2020 to 21.3 million in 2030. The Ministry of Health of the Republic of Indonesia, which has successfully collected data, shows that the prevalence of DM in Indonesia for the age limit of more than 15 years has increased by 8.5%.

Researchers around the world are still researching non-invasive methods. In recent years, research groups have conducted non-invasive research methods using infrared spectroscopy but have not shown results as accurate as invasive. By another method, the electromagnetic field interacts with an aqueous glucose solution using a microwave

dielectric waveguide probe to evaluate the glucose concentration. This technique has been used in several medical devices for detection by measuring the dielectric parameters of the biological tissue in disease diagnosis and imaging [1], [2], [3]. The ultra-wide band microwave interaction technique (UWB) has begun to be used in some medical equipment detections, because this technology is relatively inexpensive. Both in terms of financing and also have a high degree of precision [4], and currently UWB is quite widely used in medicine in detecting and monitoring tumors, cancer and so on [5], [6], [7].

One of the researchers who has conducted research with the UWB technique for the detection of blood glucose levels is Xia Xiao and Qin Wei Li et al, where the research technique was carried out using two antennas with the function of one antenna as a transmitter and the other side of the antenna as a receiver, and simulated with a tissue attached instead of earlobes, it works at a frequency of 6.5GHz. These results

simulate the measurement of blood sugar in the range 0mg/dl - 400mg/dl with a sensitivity of 50mg/dl for each change [8]. Differentiating biological cell types with microwave frequencies by identifying relative permittivity using coplanar sensors, early detection of cancer cells, imaging liver structure, and others [9]. In another study, it was reported that the dielectric size changed in solutions with different sugar concentrations [10], [11], [12].

Dielectric properties in human tissue have been characterized experimentally or in research in the frequency range 10Hz - 20GHz. Next, a parametric model was developed to describe the variation in the dielectric properties of the tissue as a function of frequency. The experimental spectrum from 10Hz to 100GHz is modeled with four dispersion areas: the Debye and the Cole-Cole models. By using the Debye model and the Cole-Cole model, dielectric parameters for human tissue with wide frequency variations can be derived for simulation models. The accuracy rate of measuring sugar levels according to the standard of medical devices is 15%, with a glucose concentration range of 50mg/dl - 80mg/dl. The lowest tolerance on the criteria for measuring blood sugar was set at ± 15 mg/dl for measurements <100mg/dl [13].

Several studies have measurements made in the frequency range between 50GHz and 75GHz. Dielectric changes occur with changes in the level of S_{21} , which were carried out with the CST-Microwave Studio Software simulation with the results of increasing the transmission amplitude to the range of 0.043dB - 0.045dB [14]. Micro-strip method with a dielectric resonator to detect sugar concentration solutions with water in the 40mg/dl - 400mg/dl range.

The Debye model was first developed to predict the permittivity value of a given glucose concentration and was proposed for glucose/water solutions in the range of 0.2GHz - 8GHz [15]. The glucose concentration sensor is designed based on an electric-LC resonator (ELC) combined with a CPW transmission line. The transmission coefficient was measured and analyzed in the 2.5GHz - 6GHz range, with an increase in transmission amplitude of 0.043dB - 0.047dB in parameter S_{21} [16]. A microwave diagnostic approach using the CPW Polymer Microwave Sensing design has been demonstrated to detect glucose levels. The measured results showed a good sensitivity of 108.4MHz/mg/ml [17].

Developed a CPW loaded with a split ring resonator (SRR) based microwave sensor to detect aqueous sucrose solutions. Analyzed in the 2GHz - 3GHz range with deionized air and water containing different sucrose concentrations from 0g/ml to 1g/ml. The amplitude increase occurred at the transmission level in the range of 7.8mdB/mgdl⁻¹ - 12.9mdB/mgdl⁻¹ [18].

Therefore, the author got the idea that microwave interaction could be used in making sensors to detect a person's blood glucose using a non-invasive method. The basis of the measurement technique is to obtain maximum interaction with the sensor in the form of a coplanar waveguide with a loaded resonator technique [19], [20]. This technique was chosen to obtain an electric field strength that can detect changes in dB levels or phase shifts by designing the placement of the test material between sensors and obtaining the best S_{11} reflection factor and S_{21} transmission factor using HFSS software. The frequency used is based on literature studies carried out, namely in the 1GHz to 6GHz

range, by varying the shape of the resonator to obtain linear changes in the S_{11} and S_{21} values and how much sensitivity they have. Hopefully, this assumption can prove and provide more in-depth knowledge about using electromagnetic waves as a non-invasive system for detecting blood sugar concentrations [21].

II. MATERIALS AND METHOD

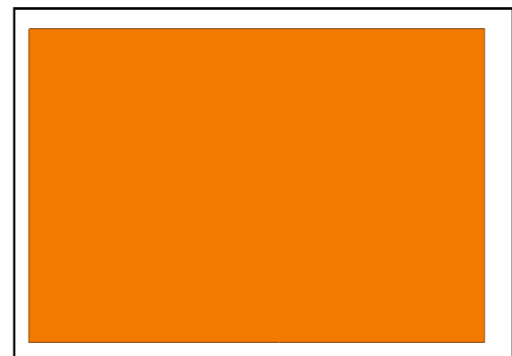
In this research, a sensor will be designed using a Printed Circuit Board type FR4 with a basic Coplanar waveguide structure. In terms of sensor design in the structure, it will be related to the determination of the working frequency and the dielectric value of a type of PCB material that will be used. The following specifications are used in designing the sensor: PCB Substrate (FR4), Dielectric material (4.4), Thickness of material (1.6mm), and Working frequency (1GHz - 6GHz).

From the results of this calculation for a working frequency of 2.8GHz, the Coplanar Waveguide dimensions are obtained as follows: Line impedance (Z_0) 50 Ω , strip width (W) 3.2mm, gap width (G) 0.5mm, relative dielectric (ϵ_r) 2.71, Physical length (λ_g) 31.5mm. In this study, modifications were made so that the sensor could detect objects on the resonator side of the CPW grounding section by maximizing the interaction of the electric field with the fingers that were censored based on microwaves. In this case, the artificial finger is modeled in the form of layers of a certain dielectric quantity. The Coplanar waveguide shape modification model is shown in Table I.

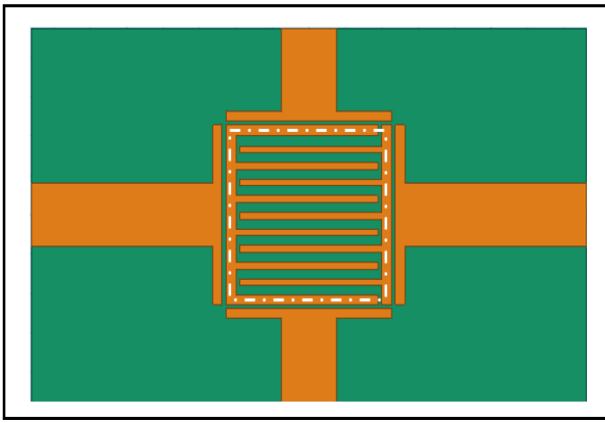
TABLE I
MODIFIED GROUND PLANE COPLANAR WAVEGUIDE

Part Model	CPW Standard	Modification
Top Surface	3 Strip Line Conductors	3 Strip Line Conductors
Substrate	1 layer	1 layer
Port	Port 1 and 2 (Scattering S_{11} and S_{21})	Port 1 and 2 (Scattering S_{11} and S_{21})
Bottom Surface/Ground Plane	Full metal conductor	Loaded as: - Square ring resonator - Interdigital capacitor - Coupling / Coupling Reinforcement

The Coplanar Waveguide sensor structure, which is made from a standard structural model and modified to become a Loaded Square Ring Resonator with an Interdigital Coupling Capacitor, can be seen in Fig. 1 (a) Standard Structure and (b) Modification Structure.



(a) Standard Structure



(b) Modification Structure

Fig. 1 (a) Standard Grounded Coplanar Waveguide. (b) Grounded Modification to Loaded Square Ring Resonator with Interdigital Coupling Capacitor

The design of the fingertips as a test material is one of the parts often used to measure blood glucose levels because it has an adequate amount of blood and a homogeneous layer of biological tissue. The fingertips will be attached to the coplanar sensor surface to implement non-invasive measurement of glucose levels in the blood. This finger tissue structure has several layers of tissue, modeled into four layers, starting with the skin, which is the outermost tissue, then fat, blood, and bone, and each of these tissues also has a certain thickness, skin (0.3mm), fat (0.2 mm), blood (1.5mm) and bone (4mm). The shape and size of the test material tissue model can be seen in Fig. 2.

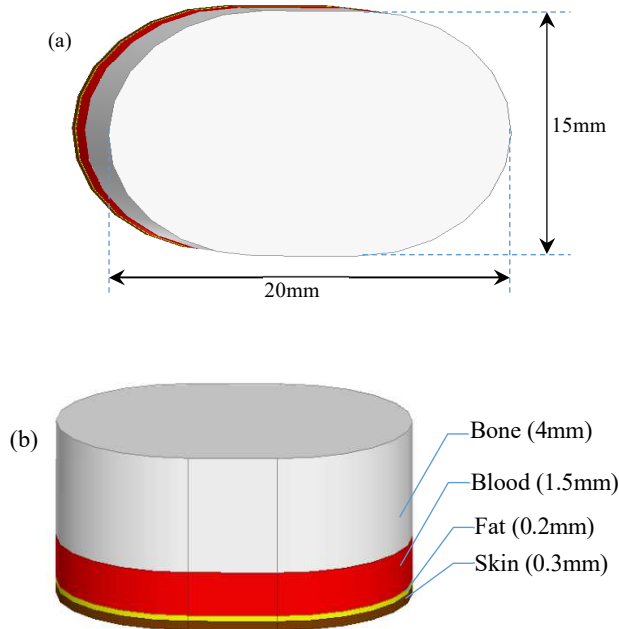
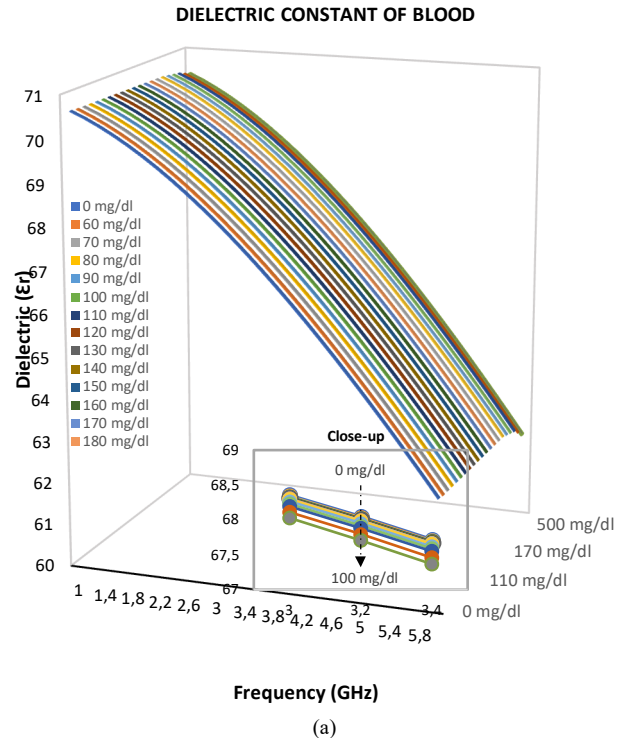


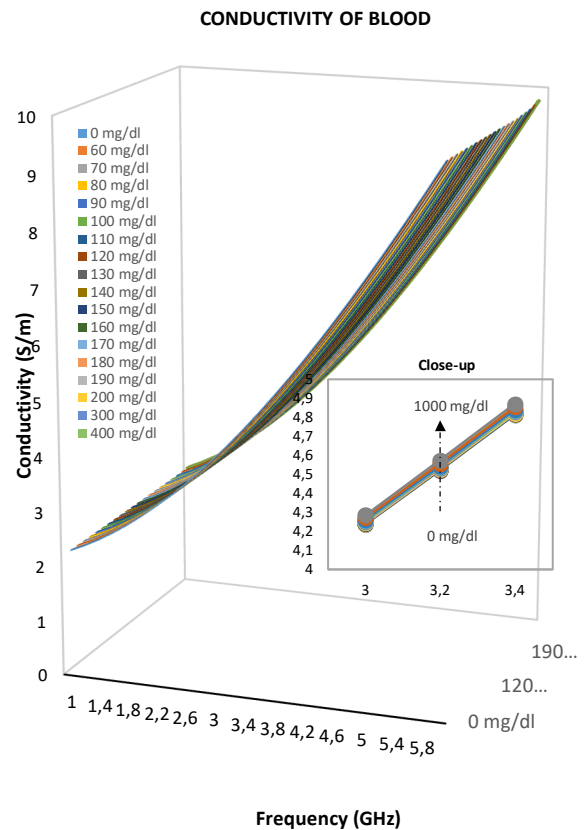
Fig. 2 (a) The length and width of the artificial finger tissue model. (b) The thickness of the artificial finger tissue layer

Body tissues used for glucose level analysis include skin, fat, blood and bone tissue with a certain dielectric quantity whose size changes at each frequency. Overall, for several body tissues, the characteristics of these changes have been studied and modeled in the form of the Cole-Cole equation

[22], [23]. In a study [24], an experiment was carried out on the relationship of electrical properties (relative permittivity, conductivity) in blood plasma and plasma glucose concentrations. Electrical properties were measured on blood samples of 10 people aged 18-40 years. The value of the dielectric quantity as a representation of the glucose level used for this simulation is given in the graph in Fig. 3.



(a)



(b)

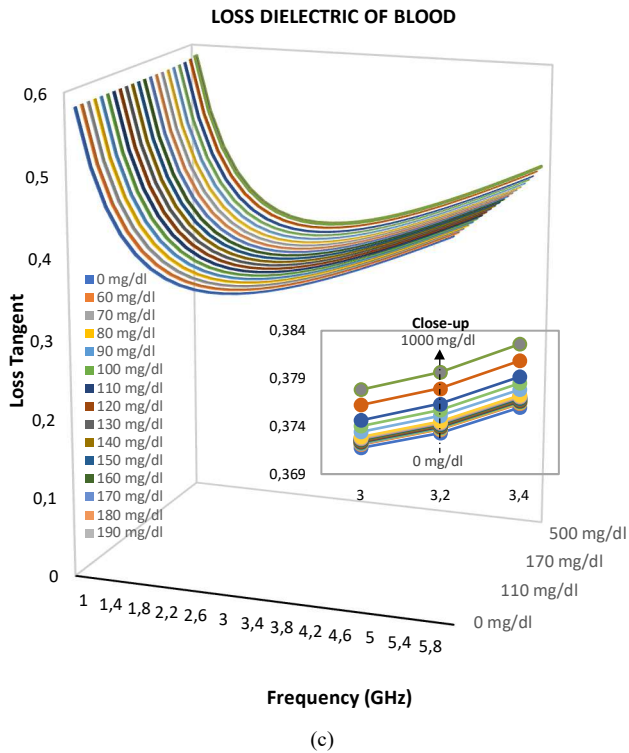


Fig. 3 Dielectric values for various blood glucose levels 0 mg/dl - 1000 mg/dl at a frequency of 1GHz - 6GHz (by calculating the Cole-Cole model); (a) Dielectric constant; (b) Conductivity; (c) Dielectric Loss

In addition to the dielectric values for blood glucose levels, a dielectric was also designed to be used to model skin, fat, and bone [25]. To get this quantity, the authors used parameters to predict the dielectric magnitude of the tissue using the Cole-Cole parameters used in table II.

TABLE II
COLE-COLE PARAMETERS FOR SKIN, FAT AND BLOOD TISSUE

Tissue	ϵ_{∞}	$\Delta\epsilon$	$\tau(\text{ps})$	σ
Skin	4	32	7.23	0.0002
Fat	2.5	3	7.96	0.01
Bone	2.5	10	1.32	0.02

The value of the dielectric quantity as a representation of the skin, fat, and bone tissue used for this simulation is given in the graph in Fig. 4.

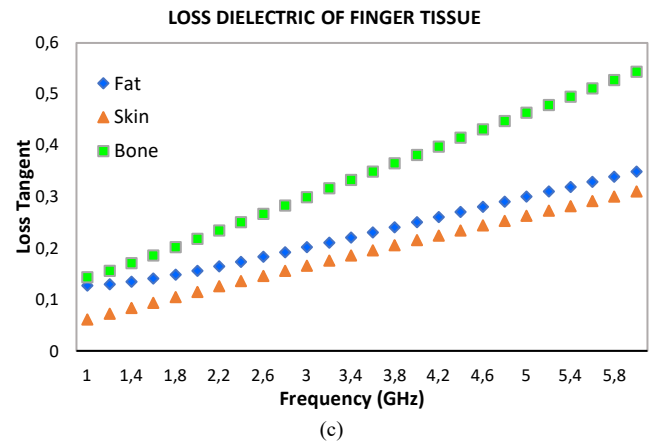
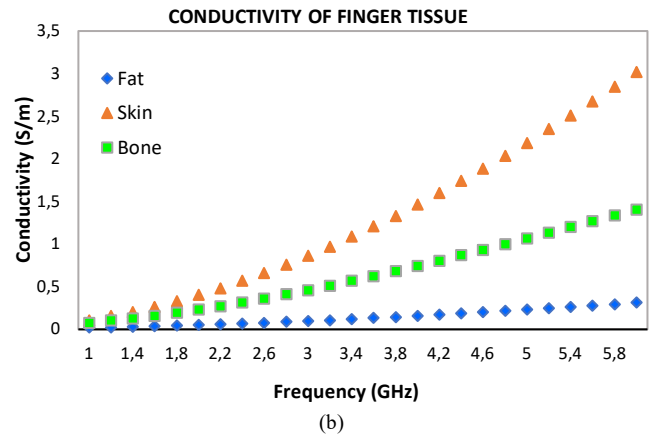
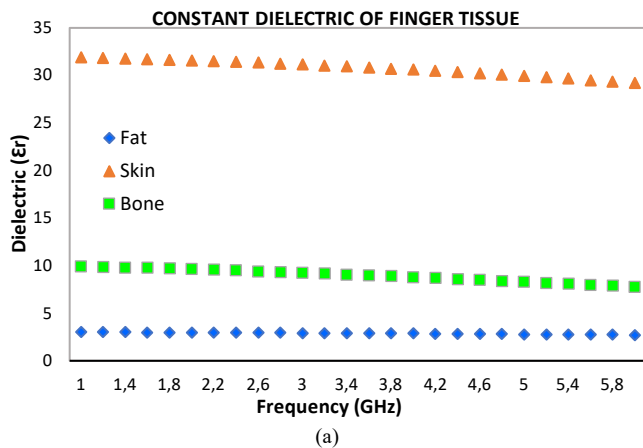


Fig. 4 Dielectric values for skin, fat, and bone in the frequency range 1GHz - 6GHz; (a) Dielectric constant; (b) Conductivity; (c) Dielectric Loss

After simulating and parametric analysis and getting the optimal sensor shape and the working frequency, fabrication is done to get the physical shape of the sensor as a representation of the simulation results. VNA measures the physical state of the sensor, and the response is analyzed with the test material. The test material made is a fingertip tissue model whose size and artificial tissue layer arrangement refer to the simulation in HFSS. The test material to be used uses gelatin as a raw material that is easily available in the market. Gelatin is often used in tissue models for simulation purposes. Making artificial tissue from gelatin material uses the method in reference [26], [27], with a mixed material composition for skin, fat, and blood tissue.

III. RESULTS AND DISCUSSION

Independent expressions of conductor thickness for the relative effective effectiveness (ϵ_{eff}) and characteristic impedance (Z_0) of the CPW with $C \rightarrow \infty$, using the conformal mapping method [28], are obtained:

- Determine the effective permittivity value (ϵ_{re})

$$\epsilon_{\text{re}} = \frac{\epsilon_r + 1}{2} \{A + B\} \quad (1)$$

Where the values A and B are the effective permittivity constants, and H is the thickness of the substrate.

- - Determine the characteristic impedance value (Z_0)

$$Z_0 = \frac{30\pi K'(k)}{\sqrt{\epsilon_{re}} K(k)} \quad (2)$$

- Determine the length value of the conductor strip (λ_g)

$$\lambda_g = \frac{300}{f(\text{GHz})\sqrt{\epsilon_{re}}} \text{ mm} \quad (3)$$

A. Analysis of Coplanar Waveguide Sensor Design with Modified Loaded Square Ring Resonator with Interdigital Coupling Capacitor (Step 1)

In this study, a sensor is designed to detect glucose levels non-invasively by observing the effect of the interaction of electromagnetic waves with matter through the basic form of Coplanar Waveguide with two ports. A standard CPW design was carried out in the early steps with theoretical-derived calculations. This calculation provides a plan for the CPW's dimensions from the substrate's type and thickness. From the calculation results, the analysis is carried out with the help of 3D High Frequency Structure Simulator (HFSS) software. This software helps analyze the resulting form in calculations to see the frequency response of the signal transmission factor S_{21} and reflection factor S_{11} .

The calculation analysis is carried out at a frequency of 3GHz because this frequency is the middle frequency of the CM Band frequency range (1GHz - 6GHz). At this frequency, modification and analysis will also be carried out to obtain a resonator shape loaded with the SRR-IDCC model [29]. Analysis of the change in the shape of the standard SRR to SRR-IDCC was carried out on several parameters, namely frequency, characteristics of the reflection factor S_{11} and transmission factor S_{21} , and the electric field of magnitude E. It was found that the defective ground area greatly influenced the reflection factor S_{11} . Parametric analysis of the capacitance area of the capacitor on the inside of the SRR ground shows that the addition of the capacitor electrode affects the S_{11} dB level, which will later be used to determine the sensitivity of the SRR-IDCC sensor level [30].

In Fig. 5, the optimization chart is shown in finding the strongest dB level, and the corresponding frequency changes are carried out in the smallest range of 0.1mm to the largest 0.5mm of the electrode width.

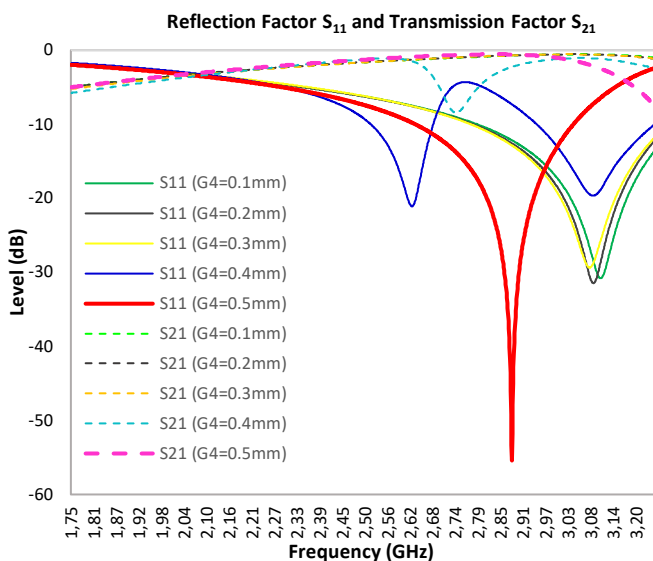


Fig. 5 SRR-IDCC optimization simulation in the range 0.1mm - 0.5mm, to determine the optimal capacitor interdigital electrode width in HFSS

The parameters of this modification and the simulation carried out in the HFSS software, the SRR-IDCC sensor structure specification, are shown in Fig. 6.

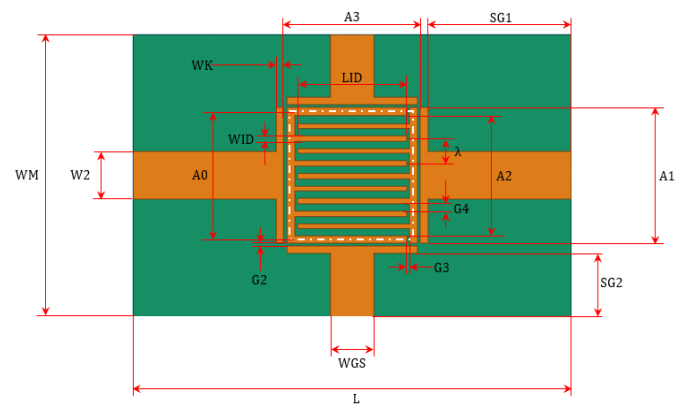


Fig. 6 Sensor parameter specifications with the SRR-IDCC structure design

The values of the geometric quantities are shown in Table III as design parameters. In Fig. 7, the optometric graph shows finding the strongest dB level, and the corresponding frequency change is carried out in the smallest range of 0.1mm to the largest range of 0.5mm of the electrode width. The most optimal results can be seen in the graph at the size of 0.3mm, namely S_{11} at the level of -55.46dB with a frequency of 2.88GHz and S_{21} at the level of -0.62dB with a frequency of 2.83GHz. The electric field (magnitude E) is shown in Fig. 8.

TABLE III
SRR-IDCC DESIGN PARAMETER SPECIFICATIONS

Bottom Sensor Size Parameters								
L	WM	A0	A1	A2	A3	SG1	SG2	
mm	mm	mm	mm	mm	mm	mm	mm	
31.5	19.2	8.2	8.7	7.7	8.9	10.8	4.65	
W2	WGS	WK	WID	LID	λ	G2	G3	G4
mm	mm	mm	mm	mm	mm	mm	mm	mm
3.2	3	0.5	0.3	7.3	1.6	0.1	0.2	0.5

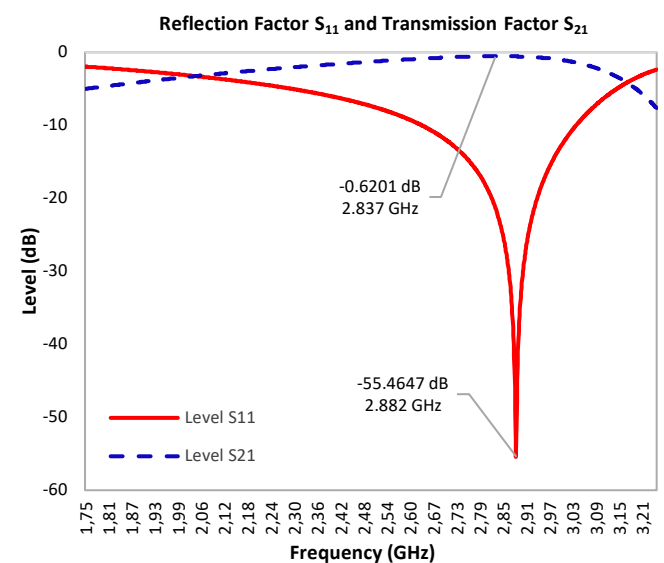


Fig. 7 Reflection Factor S_{11} and Transmission S_{21} SRR-IDCC 0.3mm capacitor interdigital electrode width with 0.5mm gap width

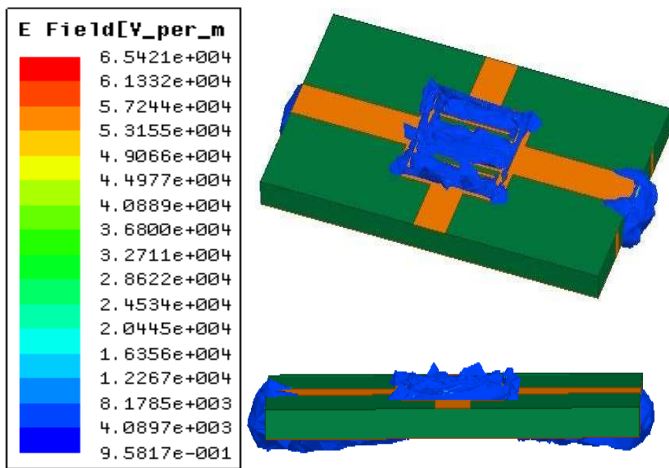


Fig. 8 Electric Field Strengthening (magnitude E) SRR-IDCC at 2.8GHz

B. Sensitivity Analysis and Optimization of Sensor with Digital Tissue in the CM Band Frequency Range of 1GHz - 6GHz (Step 2)

The sensitivity was analyzed for the test material in the 50mg/dl - 500mg/dl range with an increase of 50mg/dl. This simulation calculated the change/sensitivity value per 1mg/dl and the average yield from the range of 50mg/dl - 500mg/dl. In the middle frequency between 2.5GHz and 3GHz, there is quite a strong change in the average value of the S_{11} level. Therefore, the authors analyzed the selectivity test for wave density, a more compact analysis at frequencies between 2.5GHz - 3GHz with an increase in rate of 0.1GHz. The results of this step analysis are included in Table IV.

TABLE IV
SIMULATION RESULTS TO ANALYZE THE SENSITIVITY OF GLUCOSE LEVELS AT FREQUENCY (2.5GHz - 3GHz)

Frequency	Change in S_{11} and S_{21} Parameters in 1 mg / dl			
	S_{11}		S_{21}	
	Level (mdB/mgdl ⁻¹)	Shift (kHz/mgdl ⁻¹)	Level (mdB/mgdl ⁻¹)	Shift (kHz/mgdl ⁻¹)
2.5 GHz	0.562	2.222	0.006	0.000
2.6 GHz	9.367	0.000	0.006	2.222
2.7 GHz	0.688	0.000	0.005	0.000
2.8 GHz	64.664	0.000	0.005	0.000
2.9 GHz	0.191	0.000	0.003	0.000
3.0 GHz	0.997	0.000	0.005	0.000

From the sensitivity analysis of glucose levels at the frequency of step 2, it can be seen that in the 2.5GHz - 3GHz frequency range, the changes that occur in the frequency parameters S_{11} and S_{21} do not look significant. Significant changes occur at the dB level for the S_{11} parameter, and the largest change at each level occurs at the 2.8GHz frequency. This shows that the dB level of the S_{11} parameter at a frequency of 2.8GHz, the sensor with a CPW structure loaded Square Ring Resonator with Interdigital Coupling Capacitor has the most optimal sensitivity among other frequencies in the 1GHz - 6GHz range.

C. Simulation and Parametric Analysis Results of CPW Sensor Loaded Square Ring Resonator with Interdigital Coupling Capacitor with Digital Tissue

The sensitivity of this sensor at a frequency of 2.8GHz is shown in the graph in Fig. 9. The graph shows a relationship between changes in blood glucose concentration and S_{11}

levels; the higher the blood glucose concentration, the higher the S_{11} level.

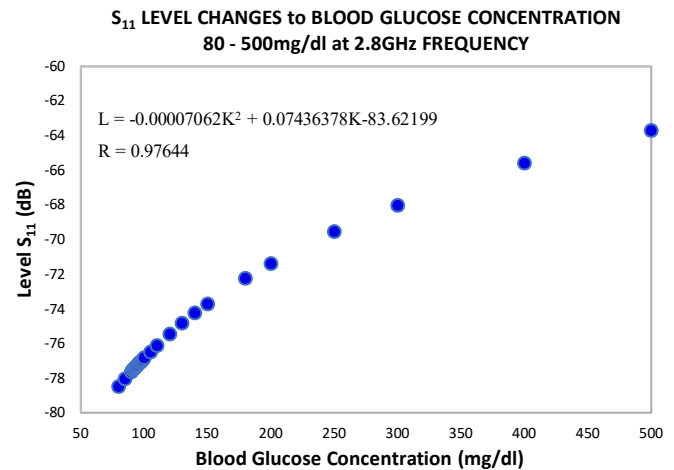


Fig. 9 Graph of the linearity sensitivity of the CPW sensor loaded with SRR-IDCC to blood glucose levels at a frequency of 2.8GHz (regression factor $R = 0.97$)

Analysis of the data on the graph between the independent variable, namely the blood glucose concentration, and the dependent variable level of S_{11} (dB) has a correlation value of $R = 0.97$. For the lowest to highest correlation scale of 0 - 1, the correlation value from the graph shows a high correlation between blood glucose concentration and S_{11} level.

Based on the analysis that has been carried out to determine the results in the form of a sensor with the highest sensitivity and according to the sensitivity correlation chart, We get the sensor from "CPW loaded Square Ring Resonator with Interdigital Coupling Capacitor", with a sensor working frequency of 2.8GHz. Analysis of the concentration of the electric field that interacts with the test material is also carried out in the sensor simulation. Using Magnitude E in the HFSS software shows the conditions of the interacting electric field and the simulation results are obtained in Fig. 10.

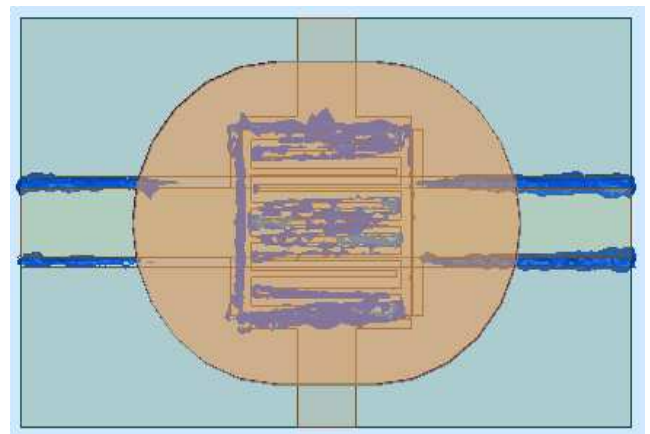


Fig. 10 The distribution of the electric field on the Grounded of CPW sensor loaded with SRR-IDCC at a frequency of 2.8GHz

Fig. 11 is the result of the signal form of the reflection factor S_{11} , which is simulated into the HFSS software. The graph shows changes in dB levels on changes in blood glucose concentrations. Reflection factor S_{11} increased dB level every time the concentration of blood glucose levels was raised.

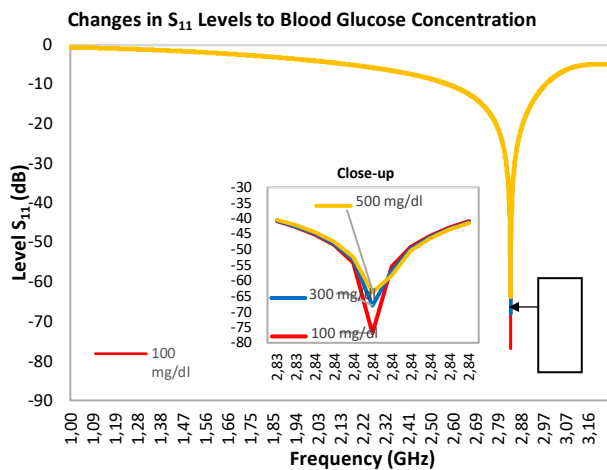


Fig. 11 Graph of changes in the reflection factor S_{11} to changes in blood glucose concentrations (100 mg/dl, 300 mg/dl, 500 mg/dl)

D. Fabrication and Result

The sensor fabrication is carried out as a representative of the analysis results carried out in a simulation using software tools after the results are obtained under the research objectives. Fig. 12 shows a physical representation of the printed form of a CPW sensor loaded with a Square Ring Resonator with an Interdigital Coupling Capacitor.

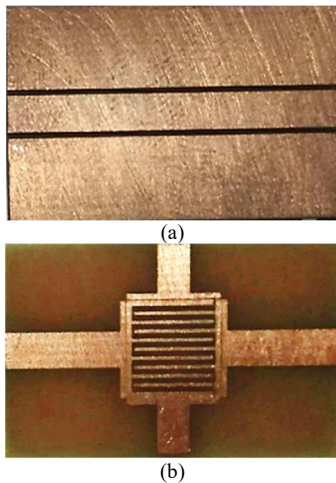


Fig. 12 PCB Fabrication Results FR4 CPW Sensor loaded with SRR-IDCC, which has been printed/etched; (a) coplanar waveguide on the front side, (b) coplanar waveguide on the back side

The PCB is then attached to port 1 and port 2 using the SMA connector on the transmission line as a connection to the VNA measuring device in the measurement process. The

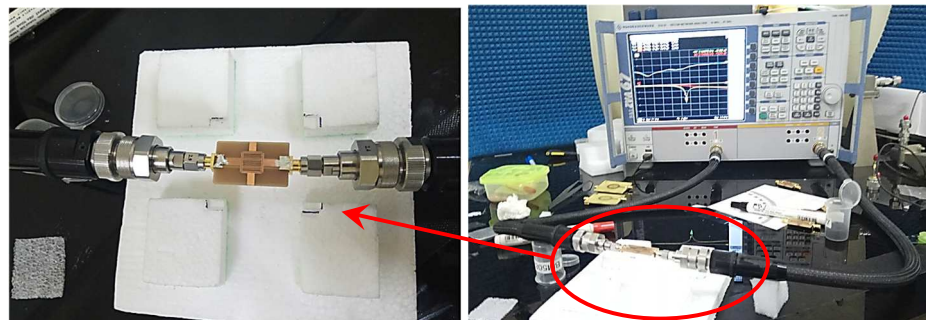


Fig. 15 Installation of measurements of CPW sensors loaded with SRR-IDCC using VNA (without test material)

connector is soldered on the terminal legs to obtain the desired signal results in monitoring the S_{11} scattering on the VNA measuring instrument.

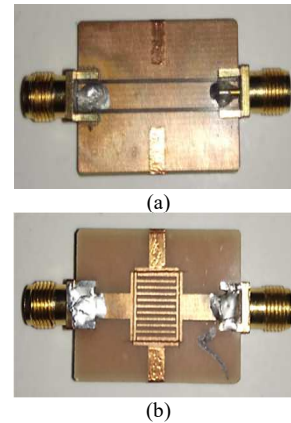


Fig. 13 PCB FR4 CPW sensor loaded with SRR with IDCC with SMA Female connector installed; (a) coplanar waveguide on the front side, (b) coplanar waveguide on the back side

The artificial finger tissue modeling fabrication is based on a principle replicating the dielectric properties of the wet skin, fat, blood, and bone in common finger pieces. RF techniques are used to measure the range of normal blood sugar levels. The composition of the artificial grid follows the literature and guidelines in reference studies, armed with the available knowledge to construct materials with a high relative dielectric constant. Fig. 14 shows the result of making artificial tissue in the form of a gel, which is processed to harden so that it can be cut into pieces using a unique cutting tool according to the size of the finger replication.



Fig. 14 Manufacture and modeling of gelatin as an artificial finger tissue

In this study, two measurements were carried out: first, the measurement of sensor fabrication results without artificial finger tissue, and second, the measurement of sensors with artificial finger tissue. In the first and second measurements, a comparison is made with the simulation results to see the suitability between the simulation and the actual measurement.

In Fig. 16, there is a combined comparison of the HFSS vs VNA measurements into one graph area of the S_{11} reflection scattering function (without test material).

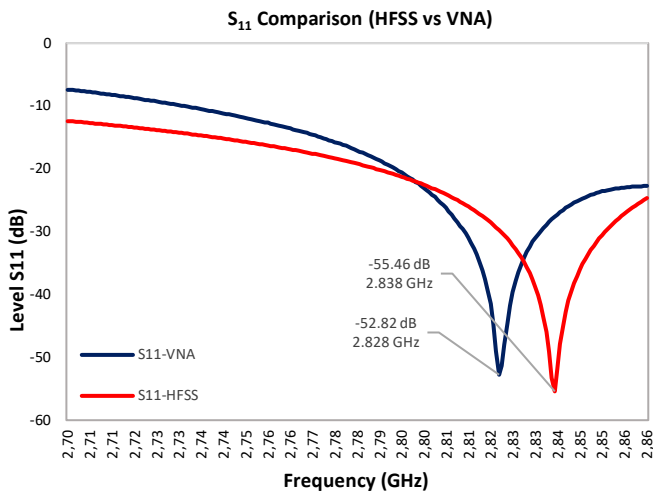


Fig. 16 Comparison graph of the measurement results of the reflection factor S_{11} (HFSS vs VNA) without the test material

Furthermore, the second stage measurement was carried out by measuring the CPW loaded SRR-IDCC sensor using the test material. A series of sensor tests with a Vector Network Analyzer, then measurements on the load are carried out by adjusting blood glucose levels with 5 test stages to determine the results of the increase in the dB S_{11} level shown on the VNA measuring instrument.



Fig. 17 Installation of measurements of CPW sensors loaded with SRR-IDCC using VNA (with test material)

These results are compared between the results obtained from the simulation and the results from the VNA measuring instrument. Blood glucose levels are 1mg/dl, 72mg/dl, 126mg/dl, 162mg/dl, and 216mg/dl. The comparative results of the sensitivity test of the CPW SRR-IDCC sensor with MUT Frequency 2.8GHz (HFSS vs VNA) were entered into Table V (HFSS) and Table VI (VNA).

TABLE V
SENSOR SENSITIVITY TEST RESULTS WITH LOAD / MATERIAL AT A FREQUENCY OF 2.8GHz (HFSS)

Step	Glucose Level	Level S_{11} (HFSS)		Deviation Glucose Level	Sensitivity mdB/mgdl^{-1}
	mg/dl	Frequency	dB		
Step 1	1	2.838	-87.6538	-	-
Step 2	72	2.838	-79.2144	71	118.86
Step 3	126	2.838	-75.1005	54	76.18
Step 4	162	2.838	-73.1181	36	55.07
Step 5	216	2.838	-70.7779	54	43.34
RATE OF SENSITIVITY					73.36

SENSOR SENSITIVITY LINEARITY GRAPH IN HFSS

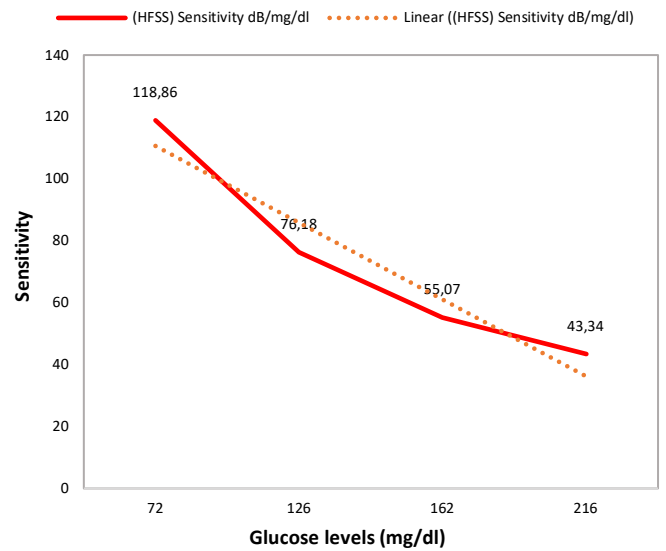


Fig. 18 Graph of sensor sensitivity linearity test results with material at a frequency of 2.8GHz (HFSS)

The following are the results of the sensor sensitivity linearity test measurement using a Vector Network Analyzer and the values are tabulated in Table VI.

TABLE VI
SENSOR SENSITIVITY TEST RESULTS WITH LOAD / MATERIAL AT A FREQUENCY OF 2.8GHz (VNA)

Step	Glucose Level	Level S_{11} (VNA)		Deviation Glucose Level	Sensitivity mdB/mgdl^{-1}
	mg/dl	Frequency	dB		
Step 1	1	2.828	-81.8054	-	-
Step 2	72	2.828	-73.362	71	118.92
Step 3	126	2.828	-67.7317	54	104.26
Step 4	162	2.828	-64.2482	36	96.76
Step 5	216	2.828	-59.281	54	91.99
RATE OF SENSITIVITY					82.39

SENSOR SENSITIVITY LINEARITY GRAPH IN VNA

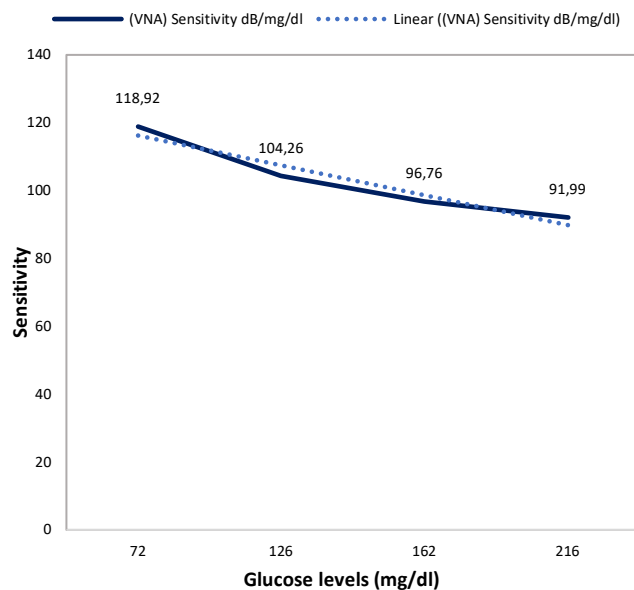


Fig. 19 Graph of sensor sensitivity linearity test results with material at a frequency of 2.8 GHz (VNA)

Sensor Sensitivity Linearity Graph (HFSS vs VNA)

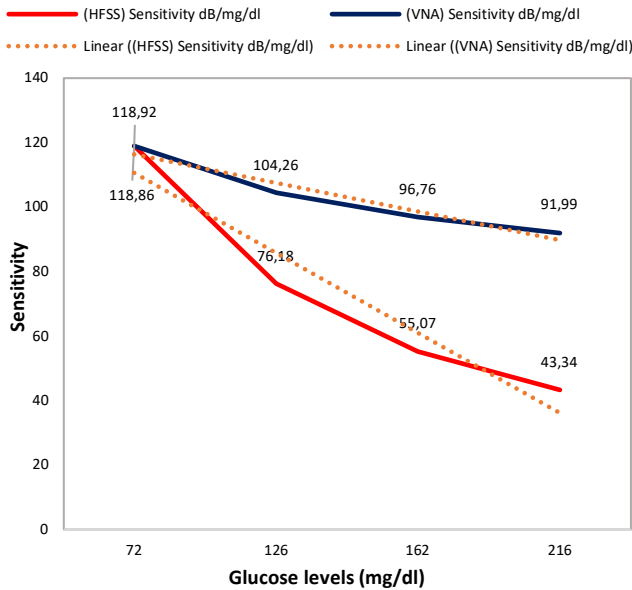


Fig. 20 Graph of the results of the linear sensitivity test for the sensitivity of the sensor with the material at a frequency of 2.8GHz (HFSS vs VNA)

The data analysis technique was carried out using a correlational relationship approach and a comparative approach (experiment). In this case, a parametric test was carried out. There is an improvement in the reflection factor S_{11} with a stable frequency position of 2.8GHz, and changes in dB levels are constant as changes are given in the form of blood glucose levels, which indicate a sensor sensitivity level of 78.18 m dB/mgdl^{-1} - 71.40 m dB/mgdl^{-1} .

The results of the data correlation analysis on the graph between the independent variables are between blood glucose concentration and the dependent variable level S_{11} . Based on the regression line equation of the curve for the level of S_{11} (L) and blood glucose concentration (K) is $L = -0.00007062K^2 + 0.07436378K - 83.62199$. Having a correlation value of R of 0.97, the correlation level in the graph shows a high correlation between blood glucose concentration and S_{11} level.

The results of the comparative data analysis represent the test comparisons between the HFSS simulation software and VNA measurements. From the comparison of simulation and measurement results, the S_{11} reflection factor is -55.46dB with a frequency of 2.838GHz, compared to the measurement of the VNA Sensor without load, the S_{11} reflection factor of -52.827dB with a frequency of 2.828GHz. Meanwhile, the comparison of simulation results and measurements with test materials at blood glucose levels of 1mg/dl, 72mg/dl, 126mg/dl, 162mg/dl, and 216mg/dl. The sensitivity level of the sensor on the reflection factor S_{11} using HFSS software was 118.86 m dB/mgdl^{-1} , 76.18 m dB/mgdl^{-1} , respectively, 55.07 m dB/mgdl^{-1} , 43.34 m dB/mgdl^{-1} , respectively. The reflection factor S_{11} using a VNA measuring instrument was 118.92 m dB/mgdl^{-1} , 104.26 m dB/mgdl^{-1} , 96.76 m dB/mgdl^{-1} , respectively, 91.99 m dB/mgdl^{-1} . The comparison results show an average sensitivity of 73.36 m dB/mgdl^{-1} to 82.39 m dB/mgdl^{-1} with a sensitivity percentage of 69.26%, so the sensor has a good linearity level between the simulation

results and the sensor fabrication results for the detection of blood glucose levels.

IV. CONCLUSION

The structure of the top three-lane Coplanar Waveguide standard ring resonator has a modified grounding side filled with a resonator (loaded resonator). The design result is a CPW-loaded square ring resonator with an interdigital coupling capacitor, which can obtain optimal electric field strengthening. The electric field that occurs in the CPW sensor loaded with SRR with IDCC is centered on the square coupling gap, which is at the center point of the lower/grounded PCB and has a good sensitivity level to the interference of the test material object that is interacted using microwaves, showing the results of the Correlation Value of 0.97. The sensitivity factor of the design results occurs in Reflection Factor S_{11} with changes in dB levels having a range of 91.99 m dB/mgdl^{-1} and can still be increased to 118.92 m dB/mgdl^{-1} in actual conditions of VNA to changes in the concentration of blood glucose levels in the range of every 1 mgdl^{-1} . The simulation results show a high sensitivity linearity level, and the measurement results suit the glucose concentration's suitability to the sensor, showing an average of 73.36 m dB/mgdl^{-1} to 82.39 m dB/mgdl^{-1} .

ACKNOWLEDGMENT

We thank Mercu Buana University, especially the microwave laboratory in Jakarta, which has contributed to providing the infrastructure for conducting research. It also shows the means of measuring sensors using a Vector Network Analyzer - VNA Rohde & Schwarz ZVA67 10MHz - 67GHz.

REFERENCES

- [1] L. Tang, S. J. Chang, C. J. Chen, and J. T. Liu, "Non-invasive blood glucose monitoring technology: A review," *Sensors (Switzerland)*, vol. 20, no. 23, pp. 1–32, 2020, doi: 10.3390/s20236925.
- [2] B. K. Mekonnen, W. Yang, T. H. Hsieh, S. K. Liaw, and F. L. Yang, "Accurate prediction of glucose concentration and identification of major contributing features from hardly distinguishable near-infrared spectroscopy," *Biomed. Signal Process. Control*, vol. 59, May 2020, doi: 10.1016/j.bspc.2020.101923.
- [3] A. S. Bolla and R. Priefer, "Blood glucose monitoring- an overview of current and future non-invasive devices," *Diabetes Metab. Syndr. Clin. Res. Rev.*, vol. 14, no. 5, pp. 739–751, Sep. 2020, doi: 10.1016/j.dsx.2020.05.016.
- [4] A. Kandwal *et al.*, "Surface Plasmonic Feature Microwave Sensor with Highly Confined Fields for Aqueous-Glucose and Blood-Glucose Measurements," *IEEE Trans. Instrum. Meas.*, vol. 70, 2021, doi: 10.1109/TIM.2020.3017038.
- [5] L. Malena, O. Fiser, P. R. Stauffer, T. Drizdal, J. Vrba, and D. Vrba, "Feasibility evaluation of metamaterial microwave sensors for non-invasive blood glucose monitoring," *Sensors*, vol. 21, no. 20, Oct. 2021, doi: 10.3390/s21206871.
- [6] D. Oloumi, R. S. C. Winter, A. Kordzadeh, P. Boulanger, and K. Rambabu, "Microwave Imaging of Breast Tumor Using Time-Domain UWB Circular-SAR Technique," *IEEE Trans. Med. Imaging*, vol. 39, no. 4, pp. 934–943, Apr. 2020, doi: 10.1109/TMI.2019.2937762.
- [7] M. K. Sharma *et al.*, "Experimental Investigation of the Breast Phantom for Tumor Detection Using Ultra-Wide Band-MIMO Antenna Sensor (UMAS) Probe," *IEEE Sens. J.*, vol. 20, no. 12, pp. 6745–6752, Jun. 2020, doi: 10.1109/JSEN.2020.2977147.
- [8] X. Xiao, Q. Yu, Q. Li, H. Song, and T. Kikkawa, "Precise Non-invasive Estimation of Glucose Using UWB Microwave with Improved Neural Networks and Hybrid Optimization," *IEEE Trans. Instrum. Meas.*, vol. 70, 2021, doi: 10.1109/TIM.2020.3010680.

- [9] A. Haider, M. U. Rahman, M. Naghshvarianjahromi, and H. S. Kim, "Time-domain investigation of switchable filter wide-band antenna for microwave breast imaging," *Sensors (Switzerland)*, vol. 20, no. 15, MDPI AG, pp. 1–10, Aug. 01, 2020, doi: 10.3390/s20154302.
- [10] M. C. Cebedio, L. A. Rabioglio, I. E. Gelosi, R. A. Ribas, A. J. Uriz, and J. C. Moreira, "Analysis and Design of a Microwave Coplanar Sensor for Non-Invasive Blood Glucose Measurements," *IEEE Sens. J.*, vol. 20, no. 18, pp. 10572–10581, Sep. 2020, doi: 10.1109/JSEN.2020.2993182.
- [11] A. E. Omer *et al.*, "Non-Invasive Real-Time Monitoring of Glucose Level Using Novel Microwave Biosensor Based on Triple-Pole CSRR," *IEEE Trans. Biomed. Circuits Syst.*, 2020, doi: 10.1109/TBCAS.2020.3038589.
- [12] S. Mohammadi *et al.*, "Gold Coplanar Waveguide Resonator Integrated with a Microfluidic Channel for Aqueous Dielectric Detection," *IEEE Sens. J.*, vol. 20, no. 17, pp. 9825–9833, Sep. 2020, doi: 10.1109/JSEN.2020.2991349.
- [13] S. Kiani, P. Rezaei, and M. Fakhr, "Dual-Frequency Microwave Resonant Sensor to Detect Non-invasive Glucose-Level Changes through the Fingertip," *IEEE Trans. Instrum. Meas.*, vol. 70, 2021, doi: 10.1109/TIM.2021.3052011.
- [14] L. Hajshahvaladi, H. Kaatuzian, and M. Danaei, "A high-sensitivity refractive index biosensor based on Si nanorings coupled to plasmonic nanohole arrays for glucose detection in water solution," *Opt. Commun.*, vol. 502, no. August 2021, p. 127421, 2022, doi: 10.1016/j.optcom.2021.127421.
- [15] M. Baghelani, Z. Abbasi, M. Daneshmand, and P. E. Light, "Non-invasive continuous-time glucose monitoring system using a chipless printable sensor based on split ring microwave resonators," *Sci. Rep.*, vol. 10, no. 1, pp. 1–15, 2020, doi: 10.1038/s41598-020-69547-1.
- [16] L. Su, J. Munoz-Enano, P. Velez, M. Gil-Barba, P. Casacuberta, and F. Martin, "Highly Sensitive Reflective-Mode Phase-Variation Permittivity Sensor Based on a Coplanar Waveguide Terminated with an Open Complementary Split Ring Resonator (OCSRR)," *IEEE Access*, vol. 9, pp. 27928–27944, 2021, doi: 10.1109/ACCESS.2021.3058575.
- [17] A. Kumar *et al.*, "High-sensitivity, quantified, linear and mediator-free resonator-based microwave biosensor for glucose detection," *Sensors (Switzerland)*, vol. 20, no. 14, pp. 1–17, Jul. 2020, doi: 10.3390/s20144024.
- [18] M. A. Zidane, A. Rouane, C. Hamouda, and H. Amar, "Hyper-sensitive microwave sensor based on split ring resonator (SRR) for glucose measurement in water," *Sensors Actuators, A Phys.*, vol. 321, Apr. 2021, doi: 10.1016/j.sna.2021.112601.
- [19] H. R. Sun *et al.*, "Symmetric coplanar waveguide sensor loaded with interdigital capacitor for permittivity characterization," *Int. J. RF Microw. Comput. Eng.*, vol. 30, no. 1, Jan. 2020, doi: 10.1002/mmce.22023.
- [20] K. Han, Y. Liu, X. Guo, Z. Jiang, N. Ye, and P. Wang, "Design, analysis and fabrication of the CPW resonator loaded by DGS and MEMS capacitors," *J. Micromechanics Microengineering*, vol. 31, no. 6, Jun. 2021, doi: 10.1088/1361-6439/abf844.
- [21] K. Abdesselam *et al.*, "A Non-Invasive Honey-Cell CSRR Glucose Sensor: Design Considerations and Modelling," *IRBM*, 2022, doi: 10.1016/j.irbm.2022.04.002.
- [22] H. Wang, L. Yang, X. Zhang, and M. H. Ang, "Results in Physics Permittivity, loss factor and Cole-Cole model of acrylic materials for dielectric elastomers," *Results Phys.*, vol. 29, p. 104781, 2021, doi: 10.1016/j.rinp.2021.104781.
- [23] S. Holm, "Time domain characterization of the Cole-Cole dielectric model," *J. Electr. Bioimpedance*, vol. 11, no. 1, pp. 101–105, Jan. 2020, doi: 10.2478/JOEB-2020-0015.
- [24] C. Cole, "Assessment of Finger Fat Pad Effect on CSRR-Based Sensor Scattering Parameters for Non-Invasive Blood Glucose," 2023, doi: 10.3390/s23010473.
- [25] A. Gorst, K. Zavyalova, and A. Mironchev, "Non-invasive determination of glucose concentration using a near-field sensor," *Biosensors*, vol. 11, no. 3, Mar. 2021, doi: 10.3390/bios11030062.
- [26] S. Costanzo, V. Cioffi, A. M. Qureshi, and A. Borgia, "Gel-like human mimicking phantoms: Realization procedure, dielectric characterization and experimental validations on microwave wearable body sensors," *Biosensors*, vol. 11, no. 4, Apr. 2021, doi: 10.3390/bios11040111.
- [27] M. Hays, S. Wojcieszak, N. Nusrat, L. E. Secondo, and E. Topsakal, "Glucose-dependent dielectric Cole-Cole models of rat blood plasma from 500 MHz to 40 GHz for millimeter-wave glucose detection," *Microw. Opt. Technol. Lett.*, vol. 62, no. 9, pp. 2813–2820, Sep. 2020, doi: 10.1002/mop.32371.
- [28] Z. Zhang and B. Zhang, "Omnidirectional and Efficient Wireless Power Transfer System for Logistic Robots," *IEEE Access*, vol. 8, pp. 13683–13693, 2020, doi: 10.1109/ACCESS.2020.2966225.
- [29] G. Crupi, X. Bao, O. J. Babarinde, D. M. M. P. Schreurs, and B. Nauwelaers, "Biosensor using a one-port interdigital capacitor: A resonance-based investigation of the permittivity sensitivity for microfluidic broadband bioelectronics applications," *Electron.*, vol. 9, no. 2, Feb. 2020, doi: 10.3390/electronics9020340.
- [30] S. Harnsoongnoen and B. Buranrat, "Advances in a Microwave Sensor-Type Interdigital Capacitor with a Hexagonal Complementary Split-Ring Resonator for Glucose Level Measurement," *Chemosensors*, vol. 11, no. 4, 2023, doi: 10.3390/chemosensors11040257.